Vision Res. Vol. 33, No. 7, pp. 861–875, 1993
Printed in Great Britain.

0042-6989/93 $6.00 + 0.00
Pergamon Press Ltd

Nonlinearity and Oscillations in X-type Ganglion Cells of the Cat Retina

A. W. PRZYBYSZEWSKI,*† M. J. M. LANKHEET,*‡ W. A. VAN DE GRIND*‡

Received 18 June 1992; in revised form 21 October 1992

Intracellularly recorded light-responses of X-type ganglion cells in the cat retina were separated, with the help of a wavelet method, into "slow" membrane ("G")-potentials and the corresponding spike trains. In response to sinusoidally modulated high intensity light spots with different sizes and frequencies, X-type ganglion cells show both oscillations correlated with the stimulus frequency and other, faster, oscillations that were not always locked to the stimulus. A forced van der Pol oscillator model with stimulus-dependent coefficients proved to describe the empirical findings quite well. A linearity-coefficient of the equations indicates strong nonlinearity at a temporal frequency of 8 Hz with spot sizes on the order of 0.5–0.7 deg and decreasing nonlinearity at lower temporal frequencies or smaller spot sizes, while the faster oscillations become more prominent. We could not determine whether the oscillations are intrinsic to the cell-membrane or generated by (or in interaction with) the preganglionic retinal meshwork. The results show that X-cell spike-trains can contain oscillations that are not phase-locked to the stimulus and that are therefore virtually invisible after stimulus synchronous averaging. It is not likely that these retinal oscillations directly induce the well described oscillations in cat visual cortex, since they usually fall in a different frequency range.

Transient oscillations Cat retina Intracellular ganglion cell recordings van der Pol oscillator

INTRODUCTION

In most neurophysiological experiments, periodic stimulation and averaging techniques are used. In such an approach one implicitly assumes that all relevant response components are synchronized with the stimulus. The application of these popular analysis methods is ineffective, however, if there exist oscillations that are not directly synchronized with the stimulus and which possibly appear only in part of the stimulation cycle. We have analysed the temporal properties of X-type retinal ganglion cells with special emphasis on the analysis of oscillations. Depending on the parameters of light stimulation two distinct oscillations were found: (1) stimulus-synchronized and (2) non-synchronized oscillations. The latter type of oscillations would be difficult to detect after response averaging, but can be seen in the raw data and in phase space plots.

It may be difficult to separate the spike generation mechanism (SGM) from the mechanism(s) responsible for ganglion cell membrane potential changes, because they may, and probably will, influence each other like a pair of coupled oscillators. In this context it is important to study the question whether there exist modes of oscillation that are evoked by, but not necessarily synchronized with, the stimulus, and to study the possibility of spontaneous oscillations in the absence of a stimulus or independent of it. If these two kinds of oscillatory phenomena exist, and we will show that they do, they provide evidence for the idea of coupled oscillators. The theme of stimulus-induced oscillations has recently gained a lot of interest because of possible implications for the "binding" or "linking" of local neuronal activities across cortical areas into a "global" message (e.g. Eckhorn, Bauer, Jordan, Brosch, Kruse, Munk & Reitboeck, 1988; Engel, König, Kreiler & Singer, 1991). We do not expand on those ideas, but find it interesting from a general neurobiological perspective that oscillations prove to be rather ubiquitous in the nervous system, if looked for. The retina appears not to be an exception, a finding that might caution against placing the burden of perception, thinking or even consciousness too one-sidedly on neuronal oscillations. Our results argue against the idea that cortical oscillations find their direct origin in the retina, because we find mostly different eigen frequencies than those reported recently on the basis of intracellular recordings in the cat's visual cortex (Jagadeesh, Gray & Ferster, 1992). However, all types of oscillations might have a similar neurobiological cause in local feedback loops and intrinsic membrane properties. From this perspective the present findings are of general interest also to those who concentrate on cortical visual mechanisms or on other species.

The present work is in some respects a continuation of our previous analysis of the SGM (Lankheet *et al.*, 1989a, b), but here we do not restrict ourselves to

*Utrecht Biophysics Research Institute, Utrecht, The Netherlands.
†To whom all correspondence should be addressed at: Department of Physiology, Freie Universität Berlin, Arnimallee 22, 1000 Berlin 33, Germany.
‡Department of Comparative Physiology, Utrecht University, Padualaan 8, 3584 CH Utrecht, The Netherlands.

averaging methods of analysis. A model of the spike generation mechanism of cat retinal ganglion cells was proposed (Lankheet, Molenaar & van de Grind, 1989a, b) based on a comparison of averaged G-potentials and averaged spike frequencies. The model accurately predicted the average spike responses from the G-potential. It was suggested that there are at least two dynamic processes underlying the SGM, one correlated with a refractory threshold with a time constant of about 0.9 msec (Hodgkin & Huxley, 1952), and another, slower threshold adaptation with a time constant of about 63 msec.

In the present paper we use different methods of analysis to show the presence of nonlinearities and oscillations in the intracellularly recorded X-type ganglion cell response to light. The spikes were subtracted with a wavelet method leaving a signal which we will call the G-potential.* We present a detailed analysis and a precise and abstract mathematical description of G-potentials in X-cells. The mathematical description is independent of any speculations on the underlying mechanisms. Even though we touch upon possible interpretations in terms of retinal network properties in the Discussion, it must be emphasized, that more and different studies are necessary to unravel the mechanistic basis of the reported nonlinearities and oscillations in X-cells.

Our mathematical (phenomenological) modelling approach is related to that of Glass and Mackey (1979) in their study of the periodic forcing of an integrate-and-fire model. In that model the authors assumed that the stimulus caused periodic changes of the threshold. Depending on the level of input activity it leads to bifurcations and to the appearance of different phase-locking zones in the relation between the input and the output of the model. However, a closer analysis of cat X-cell G-potential responses to modulated light spots with different frequencies and sizes, shows that the situation is more complex than for a periodic forcing of the integrate-and-fire model. We analysed different oscillations which are difficult to detect after averaging. They are only in part synchronized with spikes or spike bursts. Oscillations that are not synchronized with the stimulus introduce oscillations in the spike trains, which are often treated as noise in averaging methods of analysis. It will be shown that this "noise" can be increased or decreased by changing the parameters of stimulation. Such changes can be modelled using the van der Pol equation. Changing parameters of a so-called external forcing term (stimulus) in this model shows the coexistence of two different types of oscillation: one is synchronized to the stimulus and the other is non-synchronized.

*A G-potential is defined as the intracellular ganglion cell signal with the spikes subtracted as described in our Methods section. There is no generally accepted terminology for such a signal yet. "Soma" potential is unsatisfactory because we cannot be completely certain that we record from the soma rather than the axon-hillock or dendritic side of the cell. Similarly "postsynaptic" potential is unsatisfactory. "Membrane" potential often suggests some long term average or resting value and if one is prepared to use it in a more dynamic sense it should include the spikes, which the G-potential does not. "Slow" potential is clearly at variance with the relatively high frequency components and noise of the signal. "Generator" potential is suggestive enough, because we indeed refer to the signal that generates or directly underlies the spike trains, but many associate this term with receptors. Thus we compromise by using the acronym G-potential, which has the added advantage that one can read it as G(anglion cell)-potential.

METHODS

Preparation and recording

The method of animal preparation and intracellular recording has been described more extensively before (Foerster, van de Grind & Grüsser, 1977; Lankheet *et al.*, 1989a). Experiments were performed under pentobarbital anaesthesia (40 mg/kg i.p. initial dose). The cats were artificially ventilated and end-tidal PCO_2 was kept between 4 and 5%. Muscle relaxation was initiated with 80 mg flaxedil and maintained with a continuous infusion of 6.6 mg gallamine triethiodide, 0.25 mg *d*-tubocurarine and 5% glucose in 3 ml Ringer solution per hr per kg b.w. We monitored the form of the intra-aortic EKG, the (stability of the) heart rate and blood pressure. These data were used to dose additional i.v. injections of pentobarbital during the experiment. Rectal temperature was kept at about 38°C. Pupils were dilated with atropine and phenylephrine was used to retract the nictitating membrane. Lidocaine 2% was injected at all surgical sites. Ganglion cell activity was recorded intracellularly in the optically intact *in situ* eye as described before (Lankheet *et al.*, 1989a, b). The corneae were covered with contact lenses with a 1.5 × 6 mm artificial pupil. We used a stereotaxic frame that was specially developed for stable recordings from single units in the cat retina (Molenaar & van de Grind, 1980). The glass microelectrodes were filled with 4 M potassium acetate and had an impedance of 15–70 MΩ (measured with a 1 kHz square-wave signal). The recorded ganglion cell responses were amplified and fed into a tape-recorder (DTR 1800, Biologic) for off-line analysis.

Cells were classified on the basis of their response to a square-wave modulated light spot of about the size of the receptive field centre. The frequency was 0.25 Hz (alternating decrements and increments of 2 sec duration), the modulation depth was 0.6, the average luminance of the modulated spot was 53 cd/m^2 and that of the general background on the back-projection screen 0.01 cd/m^2. For our purposes it was sufficient to call a unit "sustained" or "X-type" (Enroth-Cugell & Robson, 1966) if there was a significant difference in spike frequencies measured just before the end of the increment part of the square-wave and just preceding the beginning of the decrement about 2 sec later.

Stimulation

Light sources were 450 W Xenon lamps driven by Heinzinger modulatable power supplies (bandwidth about 0–1000 Hz). The light beams passed through optical channels containing lenses, diaphragms, mirrors and filters and were focussed on a back-projection screen, having a diffuse background luminance of

0.01 cd/m^2. The spots were carefully centred on the receptive field with the help of a computer-driven "mechanical oscilloscope" (Molenaar, Voorhorst, Schreurs, Broekhuyzen, Nivard & van de Grind, 1980) and were either sinusoidally or square-wave modulated in intensity. The mean spot luminance was in the photopic range (53–530 cd/m^2), the modulation depth was 0.6 in all cases. Since the adaptation level of ganglion cells is determined by the mean flux on their receptive field (Enroth-Cugell & Shapley, 1973) we could be confident that the recorded cells were light adapted in the photopic range. This is important in classifying the cells as we did in terms of their transient-sustained character.

Data analysis

The analysis was performed on a DEC-5000 system using the Interactive Data Language (IDL). The data were sampled with 16 bits resolution at a frequency of 10 kHz. The separation of action potentials from the slower changes in the intracellularly recorded membrane potential was performed as follows. (1) The signal was convolved with a "Mexican hat" wavelet function (Przybyszewski, 1991). The width of the wavelet function was several msec and depended on the duration and shape of the action potentials. The spikes were detected and extracted by applying an interactively hand-tuned threshold to the wavelet transformation of the signal. This method is similar to the LPD (low-pass filter derivation) method (Morin-Poll & Tobin, 1991), but it is more universal because one can optimize the spike detection and extraction through the choice of the wavelet function and its duration. (2) The G-potential was extracted by removing action potentials as described above and by interpolation of the removed points by a spline function. This method is better than our previous method in which linear interpolation was used (Lankheet *et al.*, 1989a).

Hanning windowing and FFT were performed first, followed by averaging in the frequency domain. This method of analysis opens the possibility to find harmonic, subharmonic or quasiperiodic oscillations if the number of analysed periods is large enough. It is also possible to find higher frequency oscillations if phase changes from period to period are not too large. In most parts of our recordings there were oscillations that were not, or only partly, synchronized with the stimulus. They are hard to find on averaging in the frequency domain, and they are revealed more clearly in phase space.

The G-potential was drawn in a so-called pseudo three-dimensional phase space (Moon, 1987) by plotting samples of the G-potential $x(t)$ along the x-coordinate, delayed samples $x(t + \mathrm{d}t)$ along the y-coordinate and the stimulus values along the z-coordinate. The attractors in pseudo phase space have properties similar to those in classic phase space (Moon, 1987). This means that we can, for the purposes of this paper, treat our pseudo phase space plots as if they were normal phase space plots with the G-potential along the x-axis, its derivative along the y-axis and stimulus values along the z-axis. In the chosen coordinate system the structure of an attractor can only be seen for those parameters of stimulation, for which the stimulus-synchronized oscillations dominate and for which the faster nonsynchronous oscillations are not too strong. The structure of the attractor could be seen better when the x,y,z coordinate system was converted into cylindric coordinates by the following transformation:

$$u = x\cos(\omega t) - y\sin(\omega t) \quad (1a)$$

$$v = -x\sin(\omega t) - y\cos(\omega t). \quad (1b)$$

This is a natural transformation for the van der Pol equation (Hayashi, 1964).

RESULTS

Fourier analysis of the G-potential

As described in Methods, the G-potential was extracted from the intracellular potential on the basis of its shape and amplitude by using the wavelet method. Figure 1 shows examples of the intracellularly recorded ganglion (G)-cell responses to different frequencies of light stimulation from 2 Hz (top row) to 24 Hz (bottom row). For these frequencies of stimulation the size of the light spot was changed from 0.7 deg [Fig. 1(A)], to 0.5 deg [Fig. 1(B)] and 0.2 deg [Fig. 1(C)]. For each combination of frequency and spot size three traces are shown. The upper traces present the measured light response of the intracellular potential. For this particular cell the spikes had a maximum amplitude of about 45 mV (passband of the recording system 0–3 kHz). The middle traces represent the extract G-potential at a higher magnification. It can be seen (especially in the lower panels) that the interpolation with a spline function introduces minimal artefacts which are hardly visible in the G-potential traces. The occurrence of spikes does not seem to affect the G-potential very strongly and not longer than a few msec. Note that it is sometimes difficult to predict the occurrence of spikes from the modulations of the G-potential, especially for higher frequencies of stimulation.

Comparing spike trains and G-potential fluctuations in this figure, one can see that in most cases spike bursts are synchronized with the stimuli and appear during an increase or on the top of oscillations in the G-potential which is also synchronized with the stimulus. This kind of oscillation will be called a "slow oscillation". Bursts of spikes have the highest frequency and regularity in response to fast and large changes in the G-potential. This confirms previous findings (Lankheet *et al.*, 1989a, b) that spike generation seems to be more sensitive to changes of the G-potential than to its absolute value. It is also evident that, in addition to the slow G-potential fluctuation, there exist much faster changes, which are not always synchronized with the stimuli. For low frequencies of stimulation (2 or 4 Hz) their amplitude is smaller than the amplitude of the slow oscillations. In contrast, for a 24 Hz stimulus frequency, it is

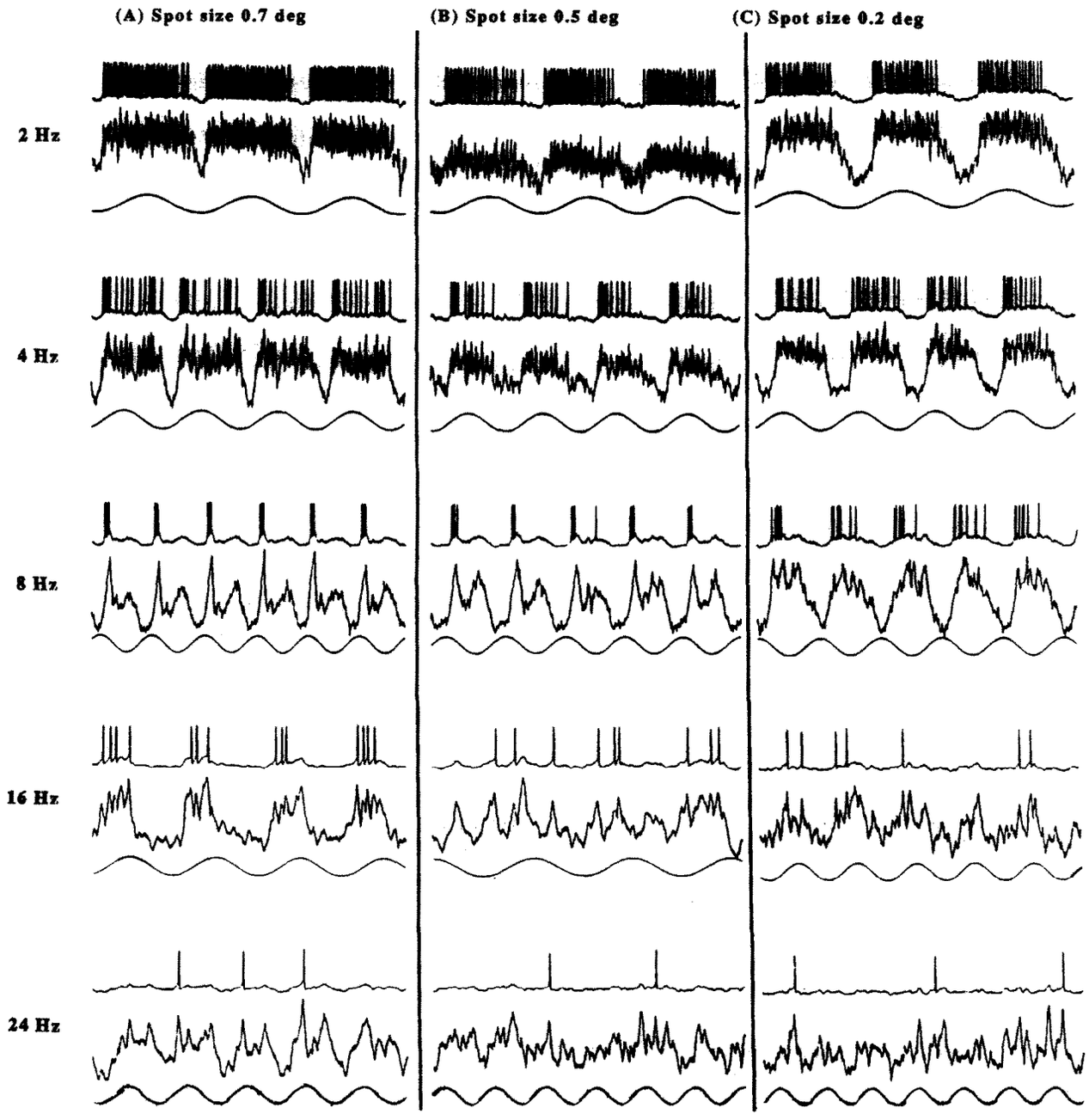

FIGURE 1. Intracellularly recorded responses from an On-centre X-type ganglion cell to sinusoidal light intensity modulation. The mean luminance was 530 cd/m^2 and the contrast was 0.6. Spot sizes and stimulus frequencies as indicated in the figure. The top trace for each stimulus condition is the recorded intracellular membrane potential. The spike amplitude in these figures is 45 mV. The middle trace represents the G-potential, i.e. the recorded membrane potential after removal of the spikes, at a higher magnification. The bottom trace shows the time-course of the light intensity modulation.

difficult to separate the modulation of the G-potential synchronized with the light stimulus from the fast and nonsynchronous oscillations. At this stimulus frequency action potentials are not generated as regularly any more as for the lower stimulus frequencies and they are not generated in every period of stimulation. Analysis of the G-potential modulations shows that there are some regularities which seem not to be correlated with spikes in such a direct way as for lower stimulation frequencies.

For a stimulus frequency of 16 Hz and a spot size of 0.7 deg, the amplitude of the slow modulation is evidently larger than that of the faster fluctuations. We interpreted this as a case in which the stimulation frequency is near the resonance frequency for slow fluctuations. This interpretation is supported by a power spectrum analysis of the G-potential (Fig. 2). For a stimulus frequency of 16 Hz, the power spectrum amplitude for the first harmonic is about ten times higher than for the other harmonics. This is not the case for other stimulation frequencies and for other spot sizes. Inspecting the power spectra for both lower (8, 4, 2, 1 Hz) and higher (24 Hz) stimulus frequencies one can always find several other peaks correlated with harmonics of the stimulus frequency. For stimulus frequencies higher than 24 Hz (not shown) the amplitude of the harmonics is very small in comparison to the other frequencies in the

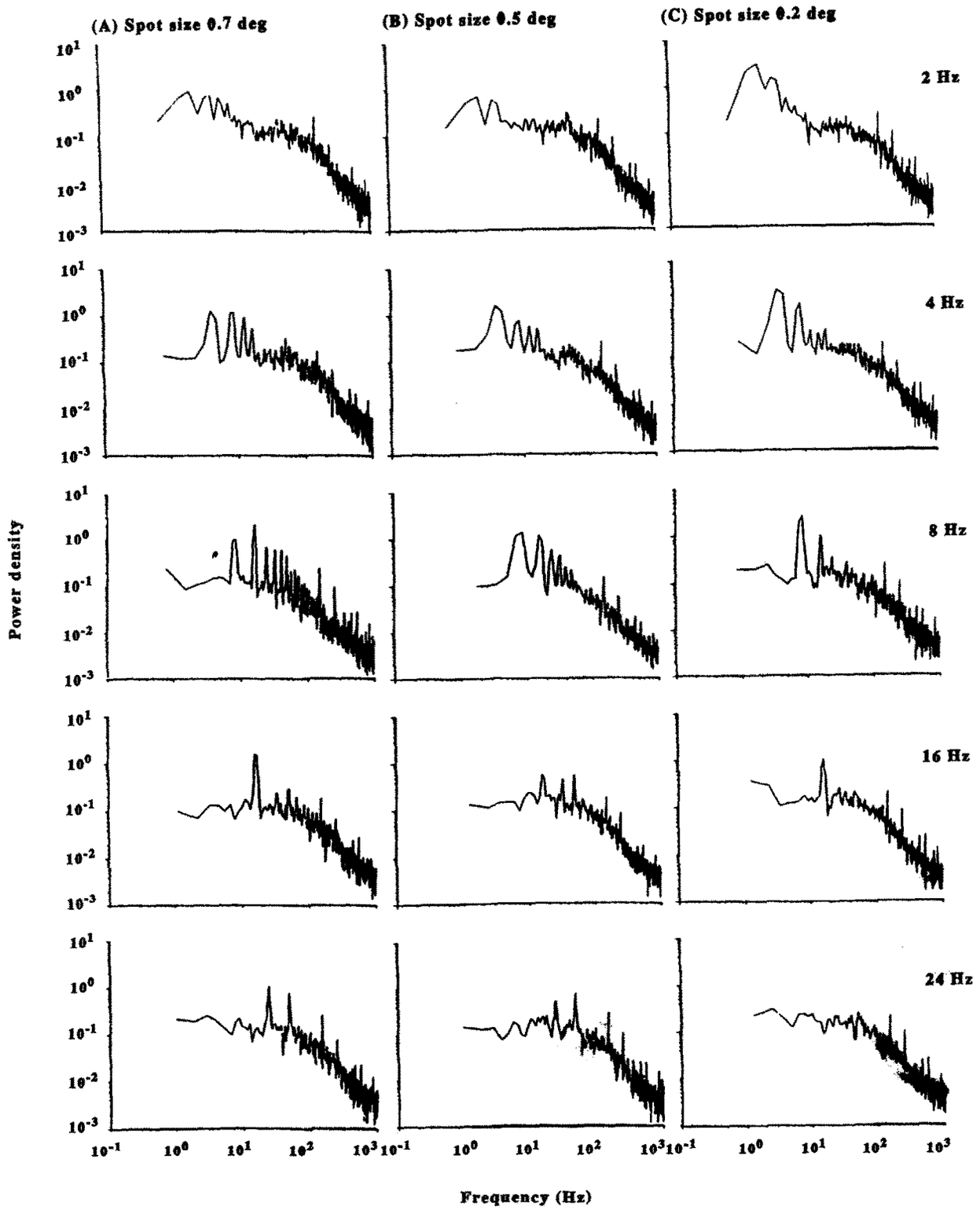

FIGURE 2. The power spectra of the G-potential for the On-centre X-type ganglion cell of Fig. 1. The stimulus parameters are equal to those in Fig. 1. Spot sizes and modulation frequencies are indicated in the figure. The G-potential was divided into several subparts, the number of which depended on the stimulus frequency. The data were Fourier analysed using the FFT after applying a Hanning window. The response parameters from the subparts were averaged in the frequency domain.

power spectrum. Decreasing the spot size from 0.7 to 0.5 deg caused the 16 Hz resonance to disappear [Fig. 2 cf. (B) to (A)]. This is also evident from the changes of the G-potential in time [Fig. 1(B)] at the stimulus frequency of 16 Hz. A further reduction of the spot size to 0.2 deg causes the 16 Hz peak to dominate in the power spectrum again. In this case stimulus-synchronized modulations are more evident in the time domain [Fig. 1(C)].

These kinds of change were also observed for other stimulation parameters and they provide evidence for nonlinearities in the retinal circuits between stimulus and G-potential. The nonlinearities could be influenced by

changing the spot size. Another example of strong changes in nonlinearity with changing spot size can be observed for 8 Hz stimulation. For larger spots (0.7 and 0.5) there are many harmonics in the power spectrum [Fig. 2(A, B)] indicating strong nonlinearities that can also be seen in the time domain [Fig. 1(A, B)]. Changing the spot size to 0.2 deg causes the stimulation frequency to dominate in the power spectrum and results in a more linear response [Figs 1(C) and 2(C)]. Notice that for this spot the spike bursting lost its regularity [cf. Fig. 1(A, B) with Fig. 1(C)]. For all frequencies of stimulation and all spot sizes the power spectrum amplitude for frequencies above 50 Hz changes with frequency in proportion to $f^{-1.5}$.

In order to study the fast oscillations in more detail the G-potential fluctuations are plotted in a pseudo three-dimensional phase space (Fig. 3). Such a plot is equivalent to a phase space plot (see Methods). Suppose the system's response to a sine wave were a pure sine wave of the same frequency again. This would lead to a circle in two-dimensional phase space (a sine along the x-axis vs a cosine on the y-axis, like a Lyssajous figure). In three-dimensional phase space this leads to an ellipsoid, the position of which depends upon the phase shift between input (z-axis) and response (x-axis). If the system now were to generate an additional higher frequency component we would get a torus in phase space. Depending on the phase relations (locked or not locked) and the frequency relationship between both response components the torus might be completely or partly covered by a space curve, the so-called trajectory. For example, at a stimulation frequency of 16 Hz in Fig. 3 these curves make large loops which are synchronized to the stimulus frequency. There are also small waves that do not exactly coincide with each other. These waves correlate with the fast oscillations in the G-potential.

Figure 3 shows responses to a sinewave flickering spot of 0.7 deg diameter and a range of frequencies from 2 to

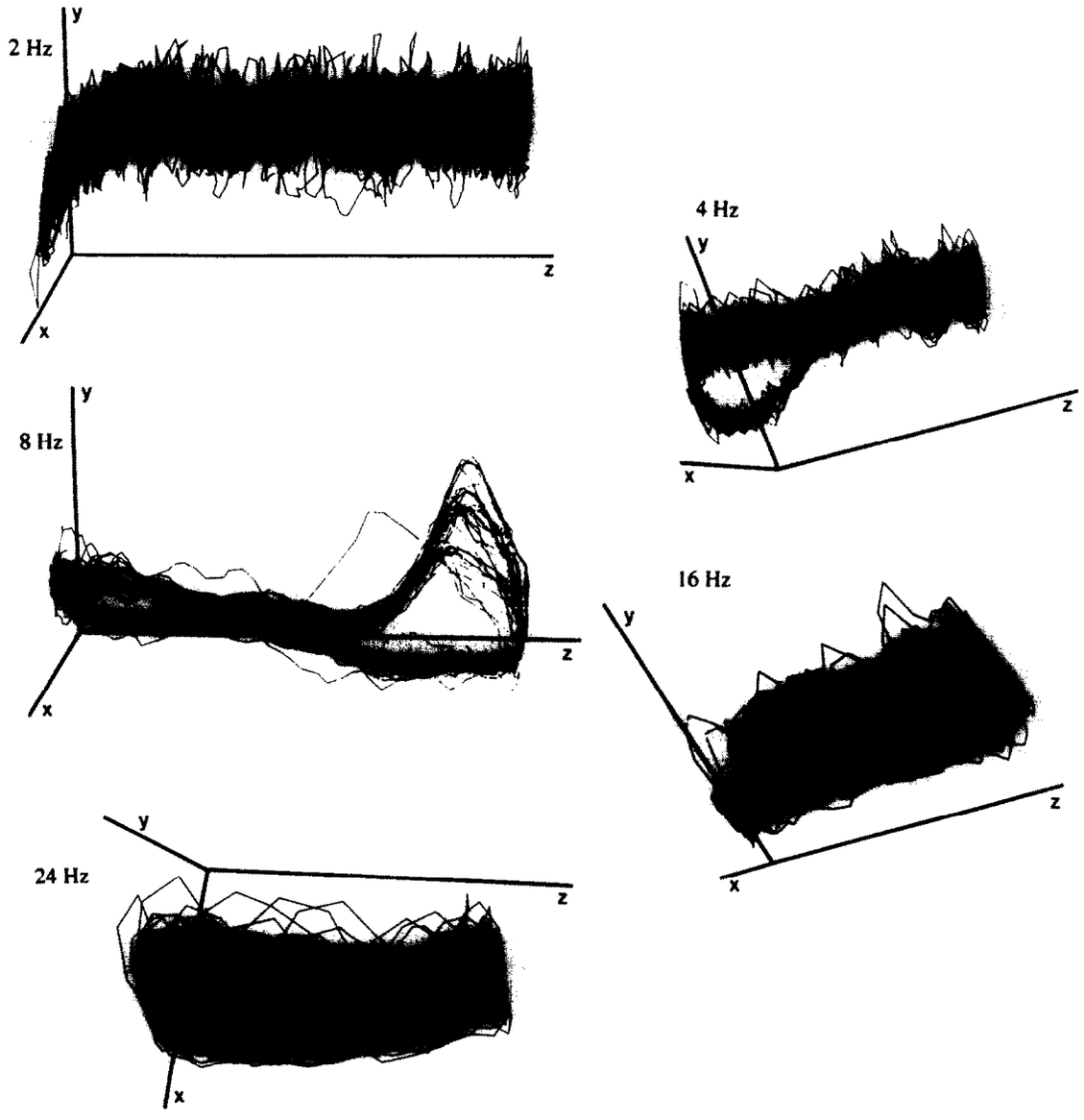

FIGURE 3. G-potentials presented in pseudo three-dimensional phase space. Shown are the responses to a light spot of 0.7 deg diameter. Stimulus frequencies are indicated in the figure. The x-, y- and z-axes represent the G-potential value, the delayed G-potential and the stimulus value, respectively. The data are normalized to the range 0–1 and oriented so as to show the shape of the attractor most clearly.

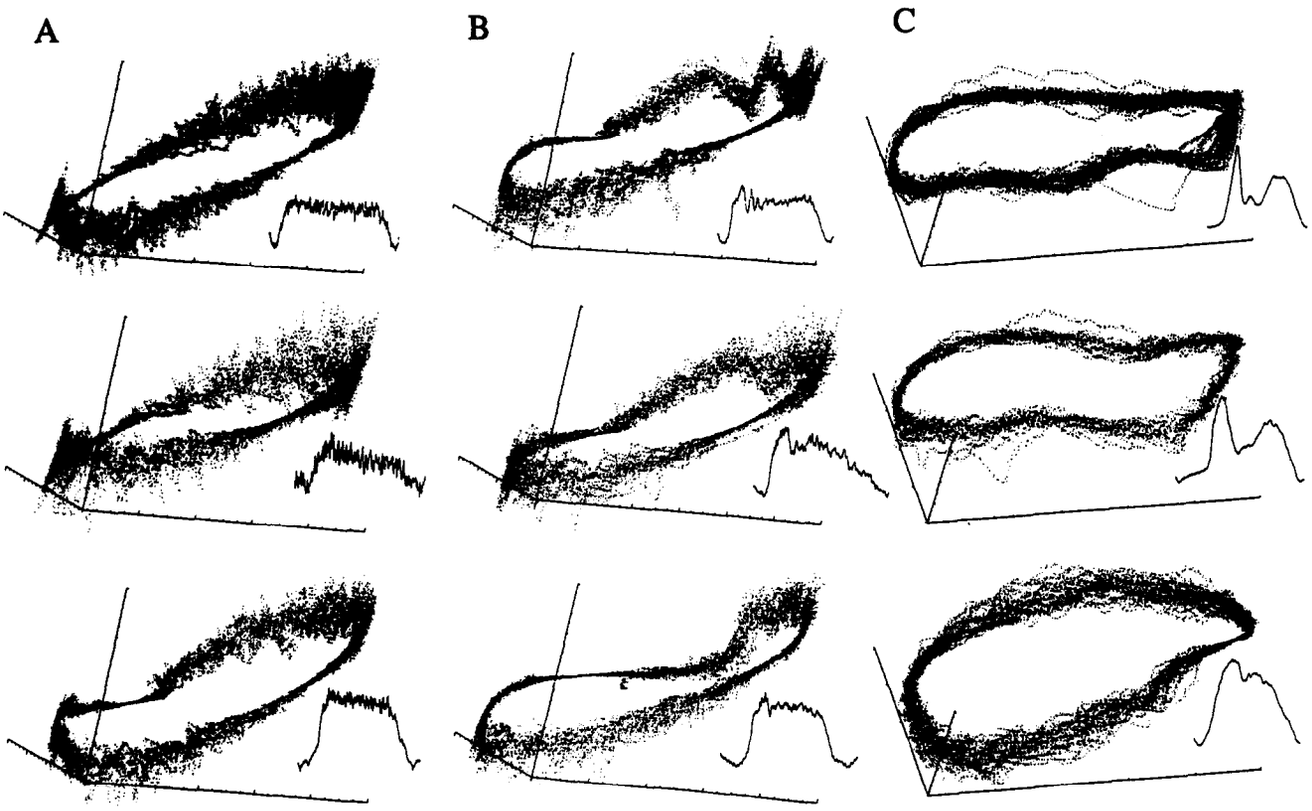

FIGURE 4. Phase space plots represented in a cylindrical coordinate system. The z-axis has the same values as in Fig. 3, but the x- and y-axes are transformed according to equations (1a) and (1b) of the text, and renormalized appropriately. The light stimulus consisted of a circular spot, sinusoidally modulated in intensity at a contrast of 0.6. The mean luminance level was 530 cd/m^2. (A) Stimulus frequency 2 Hz, (B) stimulus frequency 4 Hz and (C) stimulus frequency 8 Hz. Spot diameters: upper row, 0.7 deg; middle row, 0.5 deg; lower row, 0.2 deg. Insets in each graph present the corresponding G-potentials in the time domain, averaged over 10–50 stimulus periods, depending on the frequency of stimulation. All attractors in (A) and (B) are shown at the same orientation of the coordinate system. The attractors in (C) are tilted 50 deg further in order to show their shape more clearly. Notice the change of attractor shape with the change of spot size. In (C) the fast changes of the averaged G-potential for both a 0.7 deg (top) and a 0.5 deg (middle) spot diameter are correlated with the shape of the attractor, which is characteristic for strong nonlinearities.

24 Hz. The coordinate system has linear axes and the range is normalized. For frequencies around 4–8 Hz the structure of the attractor is clearly visible. The attractor is a locus in phase space to which most trajectories approach and it can be seen in Fig. 3 for stimulus frequencies from 4 to 16 Hz. Attractors describe dynamical equilibrium states of a system. We attempt below to develop a model, which not only mimics the changes of the G-potential in time, but also shows a similar structure of the attractor in phase space.

In Fig. 4 the linear coordinate system of the phase space of Fig. 3 was transformed into a cylindrical coordinate system, which makes it possible to see the structure of the attractor for higher and lower stimulation frequencies.

It is interesting that the thickness of the tori, which is correlated to noise or to oscillations around the tori, was much smaller for 8 Hz than for the resonance frequency of 16 Hz or for other frequencies (Fig. 3). This makes it sensible to differentiate between two kinds of oscillation: a slow oscillation with a resonance frequency of about 16 Hz, which is in most cases entrained by the frequency of stimulation and another, faster, oscillation correlated with the own (natural) frequency of the nonforced system. The faster oscillation has only one period for a stimulus frequency of 8 Hz (spot size 0.7 deg) and the number of periods increases by changing the spot size and stimulus frequency. The fast oscillations are only partly synchronized with the stimulus, as one can see by comparing the averaged G-potential to the phase space attractor. For a stimulus frequency of 16 Hz one can see in the phase space representation (Fig. 3), that the fast oscillations are not synchronized to the stimulus-entrained oscillations. For 4 Hz stimulation, there are four periods of the fast oscillations synchronized with the stimulus (Fig. 4), but the first period consists of several even faster oscillations which are non-synchronized (although they have the same frequency as the fast oscillations for the 16 Hz stimulus, i.e. about 144 Hz). For 2 Hz the situation is more complicated; there are fast oscillations (of about the same frequency of 144 Hz) and several slower, complex oscillations that are difficult to identify (Fig. 4).

For the relatively large spot size of 0.7 deg and for higher frequencies of stimulation, e.g. 24 Hz, a frequency doubling appeared [Fig. 1(A)], which dominates all other oscillations. This frequency doubling is clearly visible in the time domain as well as in the power spectrum [Fig. 2(A)]. It can also be observed for a spot size of 0.5 deg, but not for 0.2 deg [Fig. 1(B, C)]. These changes in

the G-potential are not correlated with spikes. This effect of a decorrelation between spikes and fast oscillations also takes place for a 0.2 deg spot and a 16 Hz stimulus frequency [Fig. 1(C)]. Changing the light spot size from 0.7 to 0.2 deg generally causes a stronger desynchronization of the fast oscillations which can be observed in phase space (Figs 3 and 4).

In Fig. 4 the influence of spot size change is shown more systematically in phase space for three frequencies of stimulation: 2 Hz [Fig. 4(A)], 4 Hz [Fig. 4(B)] and 8 Hz [Fig. 4(C)]. The changes in phase space can be compared to the averaged G-potential for the same parameters of stimulation (Fig. 4—insets). For a stimulus frequency of 8 Hz and a spot size of 0.7 and 0.5 deg, the increase and decrease of the slow oscillations are fast. This finds its expression in the almost rectangular shape of the attractor [Fig. 4(C), upper and middle part]. This shape is characteristic for relaxation oscillations (Grasman, 1987). A further decrease of the spot size (to 0.2 deg) caused a change in the attractor shape and in its thickness [Fig. 4(C), lower part]. For other stimulus frequencies the attractors are also rounder and only some parts of them are thin. These properties are reflected only in part in the averaged G-potential. For example, for the most nearly linear case (2 Hz, 0.5 deg) the attractor shows that there is a very regular increase and decrease of the slow potential changes from one period of stimulation to the next. This is difficult to see in the average potential. It is also impossible to say from the averaged G-potential whether the fast oscillations are synchronous with the stimulus, e.g. compare the average G-potential for stimulation with 4 Hz and a spot size of 0.7 deg with that for the other spot sizes of 0.5 or 0.2 deg.

The van der Pol oscillator as a first approximation of the G-potential responses to sinusoidal stimulation

As was mentioned previously the G-potential shows evidence of nonlinearities which are dependent on the parameters of stimulation. During darkness this cell was spontaneously discharging action potentials and its G-potential showed synchronous oscillations. The spontaneous activity indicates that the system has self-oscillatory properties. Such properties can be described by the nonlinear van der Pol differential equation. We can treat the light stimulus as the external force of the van der Pol oscillator, which is a special (simple) case of the following more general non-linear differential equation (Cartwright & Littlewood, 1945):

$$x'' + f(x)x' + g(x) = p(t) \qquad (2)$$

where f, g, p are smooth functions, $p(t)$ is the periodic external forcing term, $f(x)$ is the damping function, which should be symmetric around the origin and satisfy the condition: $f(x) > 0$ in the limit for $|x| \to \infty$. This means that the damping must be positive for large $|x|$. $g(x)$ is responsible for the "restoring" effect and should have the same sign as x.

This general equation has suitable properties for practical application because every trajectory is bounded as $t \to \infty$ (Cartwright & Littlewood, 1945). This means that for any set of initial conditions the solution of the equation, $x(t)$, stays finite. The simplest case having these properties is the van der Pol equation:

$$x'' - k(1 - x^2)x' + x = b\cos(\omega t) \qquad (3)$$

where k is a positive coefficient (not too small, e.g. 4) which determines the nonlinearity; b is the amplitude of the forcing term; $\omega = 2\pi f$, if f is the frequency of the forcing term.

We have investigated whether this relatively simple three-dimensional model can account for the observed temporal properties. More specifically, can the van der Pol equation reproduce the coexistence of stimulus-synchronous oscillations and other spontaneous oscillations which change their phase and frequency for different stimulus parameters. The following theoretical analysis of the parameter space for the van der Pol equation is based on the work of Cartwright and Littlewood (1945), Stocker (1950), Hayashi (1964), Levi (1981) and Grasman (1987).

Changing the *amplitude* b of the stimulus in a certain interval $[b_1, b_2]$ (where b_1 is small, near 0, and b_2 close to but $\frac{2}{3}$) at a constant frequency, and for large k, we can observe two alternating types of behaviour: type A is associated with a single mode, and type B with two oscillations that are different in frequency. The interval $[b_1, b_2]$ can be subdivided into a finite sequence of subintervals A_i and B_i separated by small gaps. In an interval of type B, complex irregular behaviour can also be observed. In the small gaps between the A- and B-type intervals a series of bifurcations appears. In the intervals A_i, the stable solution has a period $(2n + 1)T$, where integer $n = n(i)$ is proportional to k, and depends on the interval number of A_i. In the intervals B_i a solution with a period of $(2n - 1)T$ appears in addition to the solution with a period of $(2n + 1)T$.

By changing the *frequency* f in the forcing term relative to the natural, resonance frequency f_o (of the nonforced van der Pol oscillator)—a so-called detuning, characterized by the detuning parameter $(f - f_o)/k$—one can observe several different modes. In this case we assume a small k value, which determines "almost harmonic oscillations". In terms of the relative amplitude of the oscillations r^2 (see Stocker, 1950; Hayashi, 1964), we get complete entrainment for $r^2 > \frac{1}{2}$ (so-called phase or frequency locking). For $r^2 < \frac{1}{2}$ oscillations are doubly periodic—corresponding to the natural frequency f_o and the forcing frequency f. This leads to combined oscillations or, if f/f_o is irrational (incommensurate frequencies) it leads to quasiperiodicity, which is characterized in the Fourier spectrum by peaks for both f and f_o. When the amplitude of the forcing term is large enough, the entrained periodic solution becomes unstable and when the detuning parameter $(f - f_o)/k$ increases the other modes of oscillation will be possible. Both the natural and the forced mode will be mixed. These modes will depend on the initial conditions and a hysteresis phenomenon is observed. The other possibility is a situation where two different modes coexist. This leads

to random behaviour, which is characterized in the Poincaré section as having a strange attractor. This situation is characterized by a broad spectrum and continuous changes.

In our case we have both fast (relaxation) oscillations, which are the own oscillations of the system without a forcing term, and slow oscillations, which are synchronized and induced by the forcing term (our stimulus). The behaviour of this system depends strongly on its effective nonlinearity k, which one has to compare with some coefficient k_o, and k_o is a function of b and f (Cartwright & Littlewood, 1945). As a consequence, we can have different patterns of oscillation which are dependent on the parameters of stimulation. In the simplest case, i.e. for a stimulus frequency of 8 Hz and a large spot (0.7 deg), the fast oscillations are strongly damped and synchronized with the stimulus. In some other cases, as for stimulation at a frequency of 4 Hz, and a spot size of 0.7 deg, we also get synchronization between fast and slow oscillations, which one can see as regular peaks of fast oscillations in phase space (Fig. 4). In most cases, however, the fast oscillations are not synchronized with the stimulus. Depending on the nonlinearity parameter k the fast oscillations are either local or extend to a larger part of the stimulus period.

Simulation of the van der Pol equation

In order to investigate whether the van der Pol oscillator could describe the observed changes of G-potential dynamics for different frequencies and spot sizes we have performed numerical simulations on a digital computer (DEC 5000).

The van der Pol equation was modified in comparison to Cartwright and Littlewood (1945) and converted to two first-order equations for simulation purposes:

$$x' = k(y + x - \tfrac{1}{3}x^3) \tag{4a}$$

$$y' = -\frac{1}{k}x + a + b\cos(\omega t). \tag{4b}$$

The fourth-order Runge–Kutta method with adaptive step size was used for numerical integration of the equation. We added a bias of the forcing term by introducing a coefficient a in the above equation, where $|a| < 1$ (Hayashi, 1964). This causes a time shift of the fast oscillation relative to the slower one. In the simulations the frequency of the forcing term (light stimulus) and the values of a, b and k were changed to simulate the changes in the stimulus parameters (Fig. 1).

By choosing the coefficients of our model, it was possible to obtain:

(1) coexistence of two kinds of oscillation, a slow and a faster one;
(2) synchronization of the slow oscillation changes with the stimulus;
(3) an increase and decrease of the regularities in the fast oscillations;
(4) changing amounts of fast oscillation periods in each stimulus period;
(5) changing amplitude of the fast oscillation relative to the slower one;
(6) a characteristic change in the phase between slow and fast oscillations.

The simulation results shown in phase space (Fig. 6) exhibit a characteristic change of phase of the fast oscillation relative to the slower one which is synchronized with the stimulus. At first we fitted the parameters of the van der Pol equation to get a characteristic "one period" fast frequency excitation for the stimulation frequency of 8 Hz and a spot size 0.7 deg [Fig. 5(A)]. We obtained the following parameters: $k = 4$, $a = -0.8$ and $b = 0.8$. Decreasing the frequency of stimulation causes the fast oscillations to have more and more periods in one period of the phase locked oscillations, which is in agreement with our experimental results [cf. Fig. 1(A) for 2, 4 Hz with Fig. 5(A)]. Increasing the frequency of stimulation without changing the other parameters in the van der Pol equation would cause the fast oscillations to disappear, which is not in agreement with our results. To fit our experimental results the coefficient of nonlinearity k must be changed for different frequencies, which results in characteristic oscillations for 16 Hz and for 24 Hz [Fig. 5(A)]. But this change alone does not give the strong resonance effect observed for 16 Hz stimulation. Another coefficient, b, must be changed to get an amplitude increase in our response (b was changed from 0.8 to 1.4 for 16 Hz). For a stimulus frequency of 24 Hz and for the parameter values $b = 0.8$, $k = 1.75$ and $a = -0.8$ frequency doubling was observed in the simulations which is in agreement with the measurements.

Changes of spot size were simulated by changing the value of the nonlinearity parameter k. A decrease of the spot size is simulated in our model by a decrease of k. For 16 and 24 Hz stimulation a decrease of the light spot size from 0.7 to 0.2 deg was simulated by a change of k from 1.75 to 1.4 (0.5 deg) and 1 (0.2 deg spot size). Such changes generally result in a decrease of the damping for fast oscillations and also increase their irregularities. This can be seen both in the experimental results and in the simulation results [Figs 1(B, C) and 5(B, C)]. For a stimulus frequency of 8 Hz and a smaller spot size, the coefficient k was carefully chosen in order to obtain instabilities in the generation of one or two periods of fast oscillations: $k = 3.68$ for a spot size of 0.5 deg, and $k = 3$ for a spot diameter of 0.2 deg. For the lower frequencies of 2 and 4 Hz, the values $k = 3.7$ and $k = 3$ were used, respectively. These values of k caused an increase of the number of periods for the fast oscillations. The uniform spread of fast oscillations for the whole period was not reproducible for these simulation parameters. To simulate the decrease of the slow oscillation's amplitude, coefficient b (the effective amplitude of the stimulus) was decreased from 0.8 to 0.35. To mimic the effect that fast oscillations spread to a larger part of the slow period, coefficient a was changed. The latter coefficient can be interpreted as a threshold (or adaptation level) for the fast oscillations. Both these changes suggested that some new effects are involved for

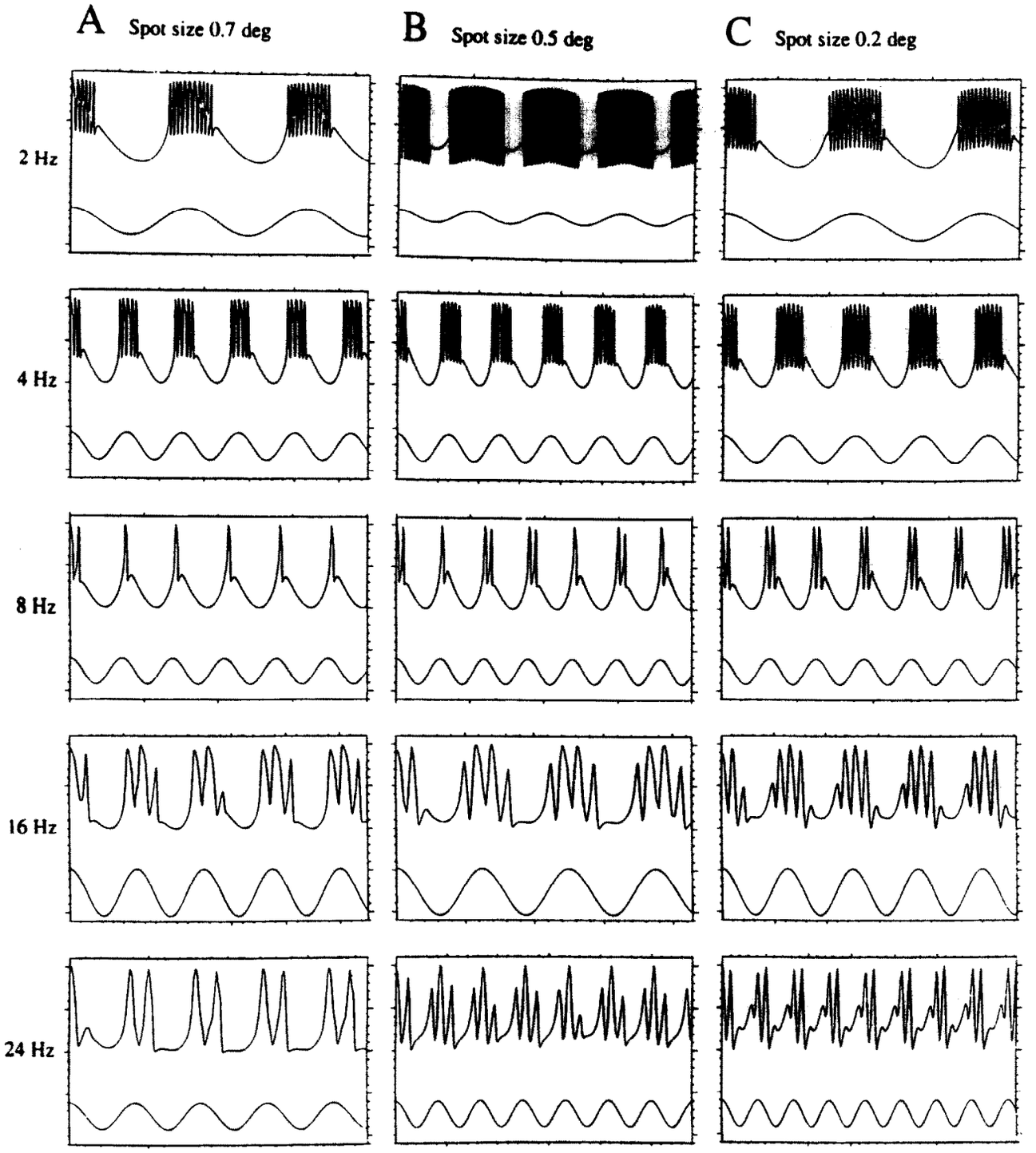

FIGURE 5. Simulation results. The van der Pol equation was used to simulate the G-potential responses of the On-centre X-type ganglion cell shown in Figs 1–4. Spot diameters and stimulus frequencies as indicated in the figure. In each box the top trace presents the simulated G-potential and the lower trace the stimulus signal.

the spot size of 0.5 deg and the frequency of 2 Hz. Decreasing the spot size to 0.2 deg causes an increase of the low frequency modulations and could be simulated with more "predictable" parameters: $b = 0.8$ and $k = 3$.

An example of the characteristic increase of the amount of fast oscillations with decreasing frequency of stimulation is shown in phase space in Fig. 6. For a stimulus frequency of 8 Hz the attractor with a shape similar to that for relaxation oscillations is presented at the bottom of the picture. The attractor is thin when it lacks the fast oscillations, and it becomes thicker even if there is only one period of the fast fluctuations. If the fast oscillations cover almost the whole period, as is shown for the model in the upper part of Fig. 6 (2 Hz stimulation, spot of 0.5 deg), the attractor becomes very thick.

DISCUSSION

Averaging methods smooth out the fast oscillations

Using Wiener's theory of non-linear analysis, Naka and Sakai (1991) interpreted their results to mean that the dynamics of the G-potential in ganglion cells is

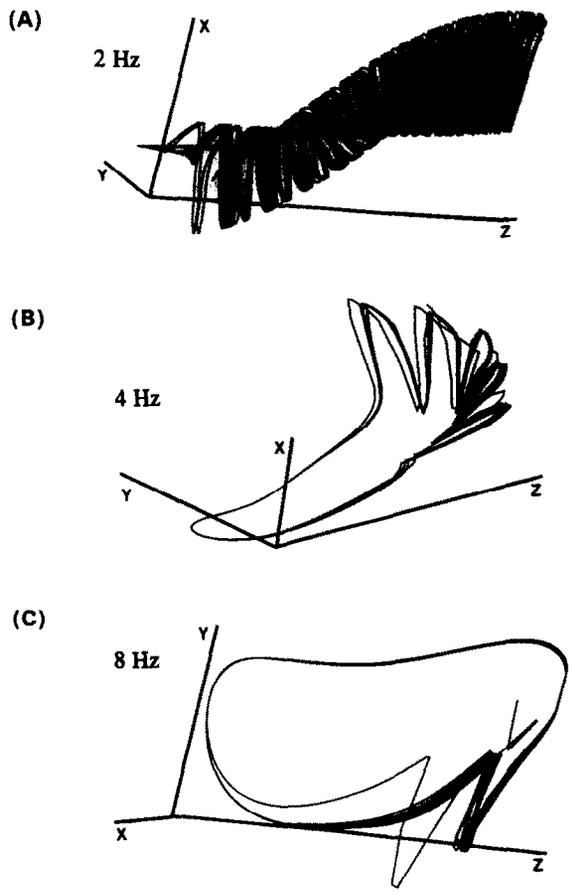

FIGURE 6. Phase space plot of the simulated G-potential. (A) Spot size 0.5 deg, stimulus frequency 2 Hz (the most linear case); (B) spot size 0.7 deg, stimulus frequency 4 Hz; (C) spot size 0.7 deg and stimulus frequency 8 Hz (the most nonlinear case). The width of the attractor can be seen to depend strongly on the parameters of stimulation.

optimal for triggering spike discharges. Lankheet *et al.* (1989b) described the possibility of inverse modelling of the spike G-potential on the basis of output spike trains. This may appear to suggest that there is no significant loss of information when the G-potential (an analogue signal) is converted into spike discharges (a point process). In a way the present analysis goes into the opposite direction, because it shows that the G-potential exhibits fast oscillations which are not always expressed in the spike trains. In most cases reported in the literature the G-potential is averaged and spike trains are summarized in the form of PST-histograms, Fourier analysis (auto-correlation), or cross-correlation (in a special case to produce a series of kernels). Averaging techniques do not preserve information about nonperiodic or local non-synchronized oscillations (see also Krüger & Becker, 1991). Power spectrum analysis (e.g. Fig. 2) can only be used to find fast oscillations in very special conditions, where they are generalized for a full period of stimulation (Przybyszewski, 1991). In our power spectra the fast oscillations are not always visible because:

(1) they are mixed with noise;
(2) they do not usually cover the full period (locality) and the power spectrum averages all frequencies within the temporal window of analysis;
(3) they are usually not locked to the stimulus, which means that they can compensate each other in the power spectrum.

The same factors obscure fast oscillations in the averaged G-potential (insets in Fig. 4). For example, one can see many small peaks in the averaged G-potential for a stimulus of 16 Hz. But these may in fact be caused by periods of strong non-synchronized fast oscillations, as is evident in the phase space plot (Fig. 3). Inspection of such oscillations can be accomplished in phase space, or by a wavelet analysis of the signal for a complete family of different filters (Przybyszewski, 1991).

Generality of fast oscillations in retinal cells

The existence of different oscillations can also be seen in other neurons by a close inspection of several figures presented in different publications: e.g. in cat ganglion cells (Lankheet *et al.*, 1989a), in amacrine cells of the cat (van de Grind, 1981) and catfish (Sakai & Naka, 1991) in ganglion and bipolar cells of the turtle (Marchiafava, 1983). The oscillations were often interpreted as frequency doubling [van de Grind, 1981; Sakai & Naka, 1990; our Fig. 1(A)], but a re-analysis of their shapes shows that there might be other causes than full-wave rectification as well [Fig. 1(A, B), 8 Hz stimulation]. Wunk and Werblin observed postsynaptic potentials in the tiger salamander retina while they polarized the ganglion cell membrane with extrinsic currents and stimulated either the centre or the surround of the cell's receptive field. During centre illumination ganglion cell responses had much stronger oscillations of the membrane potential compared with the case of illumination of the surround (Wunk & Werblin, 1979). They identified some of the peaks in the ganglion cell activity in EPSPs and IPSPs induced by bipolar cell and amacrine cell-input. There was no spike activity in their recordings because the spikes disappeared after cell preparation.

Our intracellular recordings from cat ganglion cells show clear and stable spike discharges and they therefore allow a comparison of the G-potentials and spike discharges. The fast oscillations we observed are not directly correlated with spikes, because they can be observed between spike bursts for lower frequencies of stimulation (2 Hz) as well as between spikes for higher frequencies (16, 24 Hz—different spot sizes). Thus they cannot be the direct cause of oscillations in neurons in the LGN (Podvigin, Jokeit, Pöppel, Chiz & Kiselyeva, 1992) or cortex of the cat (Jagadeesh *et al.*, 1992). Conversely, oscillations found in retinal horizontal cells of the cat retina (Foerster *et al.*, 1977) do not appear to express themselves directly at the level of the ganglion cells. This means that oscillations appear to arise *de novo* at several places along the visual pathways and might thus be a rather general phenomenon in neurons (Llinas, 1990). In this connection it is interesting that they are also found in arthropods (Kirschfeld, 1992).

Models describing oscillations in the nervous system

Hodgin–Huxley equation. Several papers describe the structure of attractors for periodically forced neural oscillations. Aihara, Matsumoto and Ikegaya (1984) and Aihara, Numajiri, Matsumoto and Kotani (1986) found synchronization, as well as quasi-periodic and chaotic oscillations in a squid giant axon stimulated by a sinusoidal current applied through an internal electrode. This behaviour could be predicted on the basis of the Hodgkin–Huxley equations (Aihara *et al.*, 1984). Similar results were obtained for an onchidium giant neuron (Hayashi, Ishizuka, Ohta & Hirakawa, 1982). It is more difficult to observe different bifurcations in the retina, because in most cases slow oscillations are synchronized with the stimulus. However, for 24 Hz we observed frequency doubling.

The integrate-and-fire model and its modification. Integrate-and-fire models are represented by first-order differential equations with a threshold (Keener, Hoppensteadt & Rinzel, 1981). The responses of such models to periodic stimuli can be: phase locking (oscillatory), aperiodic, or chaotic. In such a model the coexistence of two different stable oscillations is impossible. The same is true for the coexistence of stable phase-locked responses with different frequencies (more exactly rotation number) for certain parameter values (the hysteresis effect). In an analysis of different models for spike generation, Lankheet *et al.* (1989a) showed that the integrate-and-fire model properties do not suffice to reproduce the observed spike patterns for cat retinal ganglion cells. A major conclusion from their analysis was that at least two dynamic processes influence the firing decision.

In a frequency analysis of the G-potential we found that for spot sizes of 0.7 and 0.2 deg and a frequency of stimulation of 16 Hz the stimulus frequency dominates in the power spectrum. This can be interpreted as a resonant case. It is interesting that in the spike generating model of Lankheet *et al.* (1989a) the time constant of the slow threshold adaptation mechanism was about 63 msec, which corresponds to a frequency of around 16 Hz. This frequency is also present in our power spectra (Fig. 2) even when we used other parameters of stimulation. These findings can be interpreted as a tuning of the spike generating mechanism to the resonant frequency of some component of the retina. Similar effects of resonance were observed in other species. Power spectrum analysis of amacrine cells in catfish retina (Sakai & Naka, 1990) show that 35 Hz is a resonance frequency for these cells.

In our analysis we assume that at least two processes influence the G-potential properties. If we take the spike generating mechanism into account at least one more process, correlated with a refractory threshold, is added. It is also possible that the higher frequencies of oscillation, as observed in the power spectra, arise from an interaction between the G-potential and spike generating mechanisms. Taking the Bonhöfer–van der Pol equation (FitzHugh, 1955; Braaksma & Grasman, 1991) as a model for the spike generating mechanism we get a coupling of two nonlinear oscillators, which could cause interactions between the natural frequencies of these two systems.

van der Pol oscillator. In our experimental results we see two coexisting stable oscillations: one locked to the stimulus and the other faster and non-synchronized. We used the van der Pol oscillator as a minimal model with the properties described above. This model assumes that the unforced system has self-oscillatory properties, which in physiological terms relates to the existence of spontaneous activity in the absence of a stimulus (in darkness for on-centre ganglion cells). The coexistence of two different stable oscillations is essential for this analysis and it is an important property of the van der Pol equation. As was shown in Figs 1, 3, 4 and fast oscillations are usually not synchronized with the stimulus, so as such they are often treated as noise. Comparing the G-potential for a stimulation frequency of 8 Hz with that for other stimulus parameters shows smaller noise (Fig. 3). This fact can be seen even better in phase space, by comparing the width of the tori for different stimulation conditions. This property can be observed in our simulated *deterministic* model, where the changes of phase during stimulation are characteristic for the forced van der Pol oscillator (Fig. 6).

The slow oscillations disappear for stimulation frequencies higher than 16 Hz and for a small spot size (0.2 deg). This effect was not only observed for the frequency of 24 Hz, as shown here, but also for 32 and 40 Hz. These facts can be interpreted in terms of our model, by assuming that the higher frequencies of stimulation and the smaller spot sizes influence the system's nonlinear properties (by decreasing the coefficient k). This causes an increase of the amplitude of the natural oscillations and indirectly influences the effect of the stimulation frequency. A similar effect was observed for 2 Hz stimulation and a spot size of 0.5 deg, where the amplitude of slow oscillations suddenly becomes smaller and the fast oscillations are dominating. Decreasing the stimulation frequency from 16 Hz downwards causes many subharmonics to appear, which can be interpreted as an indirect increase in nonlinearity (we did not change k, but the influence of k also depends on ω and b). This has less influence for a 0.2 deg spot size, which supports the idea that a decrease of the spot size has a linearization influence.

By careful variation of the model parameters it proved possible to simulate some of the irregularities in the G-potential as well. As an example, compare the experimental data of Fig. 1 with the model data in Fig. 5 for a stimulation frequency of 16 Hz and a spot size of 0.5 deg. However, for some parameter values of the stimulus, e.g. 24 Hz and a spot size of 0.5 or 0.2 deg, the irregularities in the experimental data are larger than in the model. Another effect of the model that should be improved is the change in G-potential for a decreasing spot size at low frequencies of stimulation. For example, at 2 Hz a decrease of the spot size from 0.7 to 0.5 deg caused fast oscillations for the full period of stimulation (Fig. 1). This could only be mimicked very roughly by

changing coefficient a from -0.6 to -0.1 and b from 0.8 to 0.35 (Fig. 5). A similar but less severe discrepancy holds for 4 Hz. A further decrease of the spot size from 0.5 to 0.2 Hz causes another unexpected effect, viz. a change of shape of the slow G-potential oscillations. These effects are not mimicked well by our model.

We also observed higher frequencies in the power spectrum, e.g. close to the 9th harmonic of 16 Hz, which is around 144 Hz, but this is not covered by our model either. This frequency seems to be correlated with the frequency of spikes in spike bursts and their source could be a closer coupling between the SGM and the G-potential oscillator. As was discussed in the above theoretical analysis of the van der Pol equation, for some parameters of stimulation, irregular solutions exist. Such solutions are characterized by a so-called strange attractor and by broad continuous changes in power spectra. The broad-band power spectra of the G-potential [Fig. 2(A, B, C)] have a continuous fall-off which can be approximated by $f^{-1.5}$. This property may be caused by noise or by a chaotic process. The $f^{-1.5}$ power law might be interpreted as the self similar variation on different time scales, which is correlated with a fractal process (Goldberger & West, 1987).

Comparison with extracellular recordings from ganglion cells

The present results emphasize an aspect that has hitherto been covered, but they are otherwise in general agreement with other findings on the G-potential or extracellular spike response of cat ganglion cells. For example Lankheet *et al.* (1989a, b) report that the amplitude of the first harmonic of the G-potential (the slow stimulus-locked oscillations) has a maximum at a temporal frequency of around 16 Hz for larger spot sizes and at lower frequencies for smaller spot sizes. Frishman, Freeman, Troy, Schweitzer-Tong and Enroth-Cugell (1987), recording from the optic tract, used gratings as a stimulus under photopic conditions. They found that the X-cell's responsivity was essentially constant at temporal frequencies from 1.5 to about 39 Hz. Derrington and Lennie (1982) reported that the sensitivity at the optimum spatial frequency was higher at a temporal frequency of about 10 Hz than at lower or higher temporal frequencies. Grüsser (1971) found that photopic stimulation of the receptive field centre with sinusoidally modulated small light spot(s) gives maximum responses for frequencies between 8 and 12.5 Hz. If the size of the stimulating spots (the stimulation area) in the receptive field centre decreases, the response amplitude also decreases but not in a linear manner. Grüsser (1971) found a hysteresis effect during continuous increase and decrease of the light spot diameter. The response amplitude depended on the direction of change. These results support the idea that clear nonlinearities exist in the receptive field centre of cat ganglion cells.

Enroth-Cugell and Robson (1966) proposed the classification of ganglion cells into X- and Y-types on the basis their linear (nonlinear) spatial summation properties for appropriate spatial and temporal frequencies and a relatively low contrast. On the basis of our recordings and simulation of the G-potential it appears that X-type ganglion cells also show nonlinearities. These nonlinearities, which are visible in the temporal structure of the soma potential, depend on the stimulation parameters. Not only contrast but also spot size (spatial frequency) and temporal frequency of stimulation are important. X-centre ganglion cells may evoke at least two different kinds of oscillation. The first one, their own or natural frequency is correlated with properties of retina circuitry in the stimulus-free situation. These oscillations are called "fast" in this paper. They are relaxation oscillations, which can be best observed for 24 Hz stimulation [Fig. 1(A)]. The shape of the "slower" oscillations, depends more strongly on the parameters of stimulation. The slower oscillations are relaxation oscillations for 8 Hz [0.7 or 0.5 deg spot size—Figs 1(B, C) and 4] but a decrease in stimulation frequency and spot size increases their linearity [Fig. 1(B, C)].

Strong nonlinear oscillations of the G-potential can possibly be detected in extracellular recordings on the basis of bursting. Burst regularity may also be analysed with the wavelet method (Przybyszewski, 1991). This kind of analysis has a physiological meaning. One may assume that an important role of X-type cells is to encode a precise message about contrast, spatial and temporal properties of the stimulus. If the stimulus tunes in with the resonance of X-cell circuity (for the fast oscillation type), the G-potential has its maximum nonlinear shape, which can cause a high speed threshold crossing and thus generate a relatively precise timing of spike bursts. Such a message or coding mechanism (Koenderink & van Doorn, 1973) might be repeated on higher levels and will be resistive to random fluctuations.

Possible anatomical and physiological basis of G-potential oscillations

Some or all of the uncovered oscillations might be caused by intrinsic properties of the ganglion cell membrane. However, it seems more likely that at least some of the oscillations are network properties. There are several feedback loops in the retina that might be a source of oscillations under specific circumstances or for a specific combination of stimulus parameters. These include: (1) feedback from horizontal cells to cone-pedicles (Chun & Wässle, 1989); (2) feedback from amacrine cells to bipolar cells or reciprocal connections in the inner plexiform layer (Kolb, Nelson & Marianni, 1981); (3) feedback from the inner plexiform layer to the outer plexiform layer through interplexiform cells (Kolb & West, 1977). It has been suggested that the small oscillations of about 40 Hz which can often be found in cone-dominated horizontal cells are a consequence of the first mentioned feedback circuit (Foerster *et al.*, 1977). In view of their properties (*op cit*) we assume that if they play a role at the level of ganglion cells it is probably a minor one that can only be uncovered by high intensity, high temporal contrast, large-field stimulation. The third possibility is very hard to evaluate at present, because nothing is known about the physiological properties of

interplexiform cells. Perhaps loops at or near the ganglion cell in the inner plexiform layer are the safest bet. The oscillations in G-potentials might be the result of complex interactions between different subsystems like membranes, cells or small neural networks (cell assemblies), with stimulus-dependent shifts in dominance. The functional properties of these subsystems can probably be studied in more detail with a generalization of the method developed by Hochstein and Shapley (1976) to analyse the subunit structure of Y-type ganglion cell receptive fields.

In conclusion, our results show that the G-potential oscillates in various modes which are dependent on the stimulus parameters. A description in terms of a forced van der Pol oscillator summarizes many of the intricate oscillatory properties of the G-potential. Oscillatory behaviour of this type or variants of it are probably ubiquitous in the nervous system, which means that the proposed description might have a more general validity. As far as the retina is concerned one would eventually want an explanation in more mechanistic terms, which will probably require neuropharmacological experiments to selectively suppress some of the many retinal feedback loops. The retina might prove to be a good model for the study of oscillatory phenomena, since it is accessible and well-studied in other respects.

REFERENCES

Aihara, K., Matsumoto, G. & Ikegaya, Y. (1984). Periodic and non-periodic responses of a periodically forced Hudgkin–Huxley oscillator. *Journal of Theoretical Biology, 109*, 249–269.

Aihara, K., Numajiri, T., Matsumoto, G. & Kotani, M. (1986). Structures of attractors in periodically forced neural oscillators. *Physics Letters A, 116*, 313–317.

Braaksma, B. & Grasman, J. (1991). Critical dynamics of the Bonhöffer–van der Pol equation and its chaotic response to periodic stimulation. *Physica D*, to appear, preprint 669, Department of Mathematics, Utrecht University, The Netherlands.

Cartwright M. L. & Littlewood, J. E. (1945). On nonlinear differential equations of the second order. I The equation $y'' - k(1 - y^2) y' + y = b\lambda k \cos(\lambda t + \alpha)$, k large. *Journal of the London Mathematical Society, 20*, 180–189.

Chun, M. H. & Wässle, H. (1989). GABA-like immunoreactivity in the cat retina: electron microscopy. *Journal of Comparative Neurology, 279*, 55–67.

Derrington, A. M. & Lennie, P. (1982). The influence of temporal frequency and adaptation level on receptive field organization of retinal ganglion cells in cat. *Journal of Physiology, London, 333*, 343–366.

Eckhorn, R., Bauer, R., Jordan, W., Brosch, M., Kruse, W., Munk, M. & Reitboeck, H. J. (1988). Coherent oscillations: A mechanism of feature linking in the visual cortex? *Biological Cybernetics, 60*, 121–130.

Engel, A. K., König, P., Kreiter, A. K. & Singer, W. (1991). Interhemispheric synchronization of oscillatory neuronal responses in cat visual cortex. *Science, 252*, 1177–1179.

Enroth-Cugell, C. & Robson, J. G. (1966). The contrast sensitivity of retinal ganglion cells of the cat. *Journal of Physiology, London, 187*, 517–552.

Enroth-Cugell, C. & Shapley, R. M. (1973). Flux, not retinal illumination, is what cat retinal ganglion cells really care about. *Journal of Physiology, London, 233*, 311–326.

FitzHugh, R. (1955). Mathematical models of threshold phenomena in the nerve membrane. *Bulletin of Mathematical Biophysics, 17*, 257–278.

Flaherty, J. E. & Hoppensteadt, F. C. (1978). Frequency entrainment of a forced van der Pol oscillator. *Studies in Applied Mathematics, 58*, 5–15.

Foerster, M. H., van de Grind, W. A. & Grüsser, O.-J. (1977). Frequency transfer properties of three distinct types of cat horizontal cells. *Experimental Brain Research, 29*, 347–366.

Frishman, L. J., Freeman, A. W., Troy, J. B., Schweitzer-Tong, D. E. & Enroth-Cugell, C. (1987). Spatiotemporal frequency responses of cat retinal ganglion cells. *Journal of General Physiology, 89*, 599–628.

Glass, L. & Mackay, M. C. (1979). A simple model for phase locking of biological oscillators. *Journal of Mathematical Biology, 7*, 339–352.

Goldberger, A. L. & West, B. J. (1987). Fractals in physiology and medicine. *Yale Journal of Biology and Medicine, 60*, 421–435.

Grasman, J. (1987). *Asymptotic methods for the relaxation oscillations and applications*. New York: Springer.

van de Grind, W. A. (1981). Intracellular recording studies of visual signal processing in the cat retina. *Documenta Ophthalmologica Proceedings Series, 30*, 21–30.

Grüsser, O.-J. (1971). A quantitative analysis of spatial summation of excitation and inhibition within the receptive field of the retinal ganglion cells of cat. *Vision Research (Suppl.), 3*, 103–127.

Hayashi, C. (1964). *Nonlinear oscillations in physical systems*. New York: McGraw-Hill.

Hayashi, H., Ishizuka, O., Ohta, M. & Hirakawa, K. (1982). Chaotic behaviour in the onchidium giant neuron under sinusoidal stimulation. *Physics Letters A, 88*, 435–438.

Hochstein, S. & Shapley, R. M. (1976). Linear and nonlinear spatial subunits in Y cat retinal ganglion cells. *Journal of Physiology, London, 262*, 265–284.

Hodgkin, A. L. & Huxley, A. F. (1952). A quantitative description of membrane current and its application to conduction and excitation in nerve. *Journal of Physiology, London, 117*, 500–544.

Jagadeesh, B., Gray, C. M. & Ferster, D. (1992). Visually evoked oscillations of membrane potential in cells of cat visual cortex. *Science, 257*, 552–554.

Keener, J. P., Hoppensteadt, F. C. & Rinzel, J. (1981). Integrate-and-fire models of nerve membrane response to oscillatory input. *SIAM Journal of Applied Mathematics, 41*, 503–517.

Kirschfeld, K. (1992). Oscillations in the insect brain: Do they correspond to the cortical γ-waves of vertebrates? *Proceedings of the National Academy of Science U.S.A., 89*, 4764–4768.

Koenderink, J. J. & van Doorn, A. J. (1973). Event train decoders with many inputs, pulse density versus momentaneous frequency. *Kybernetik, 13*, 215–222.

Kolb, H. & West, R. W. (1977). Synaptic connections of the interplexiform cell in the retina of the cat. *Journal of Neurocytology, 6*, 155–170.

Kolb, H., Nelson, R. & Marianni, A. (1981). Amacrine cells, bipolar cells and ganglion cells of the cat retina: A Golgi study. *Vision Research, 21*, 1081–1114.

Krüger, J. & Becker, J. D. (1991). Recognizing the visual stimulus from neuronal discharges. *Trends in Neuroscience, 14*, 282–286.

Kuffler, S. W. (1952). Neurons in the retina: Organisation, inhibition and excitation problems. *Cold Spring Harbor Symposium on Quantitative Biology, 17*, 281–292.

Lankheet, M. J. M., Molenaar, J. & van de Grind, W. A. (1989a). The spike generation mechanism of cat retinal ganglion cells. *Vision Research, 29*, 505–517.

Lankheet, M. J. M., Molenaar, J. & van de Grind, W. A. (1989b). Frequency transfer properties of the generating mechanisms of cat retinal ganglion cells. *Vision Research, 29*, 1649–1661.

Levi, M. (1981). Quantitative analysis of periodically forced relaxation oscillations. *Memorandum of the American Mathematical Society, 32*, 147.

Llinas, R. (1990). Intrinsic electrical properties of nerve cells and their role in network oscillation. *Cold Spring Harbor Symposia on Quantitative Biology, LV*, 933–938.

Marchiafava, P. L. (1983). The organization of inputs establish two functional and morphologically identifiable classes of ganglion cells in the retina of the turtle. *Vision Research, 23*, 325–338.

Marion-Poll, F. & Tobin, T. R. (1991). Software filter for detecting spikes superimposed on a fluctuating baseline. *Journal of Neuroscience Methods, 37*, 1–6.

Molenaar, J. & van de Grind, W. A. (1980). A stereotactic method of recording from single neurons in the intact *in vivo* eye of the cat. *Journal of Neuroscience Methods, 2*, 135–152.

Molenaar, J., Voorhorst, R., Schreurs, A. W., Broekhuyzen, P., Nivard, J. & van de Grind, W. A. (1980). A mechanical oscilloscope for vision research. *Pflügers Archiv, 383*, 173–179.

Moon, F. C. (1987). *Chaotic vibrations. An introduction for applied scientists and engineers.* New York: Wiley.

Naka, K.-I. & Sakai, H. M. (1991). The messages in optic nerve fibers and their interpretation. *Brain Research Review, 16*, 135–149.

Podvigin, N. F., Jokeit, H., Pöppel, E., Chizh, A. N. & Kiselyeva, N. B. (1992). Stimulus-dependent oscillatory activity in the lateral geniculate body of the cat. *Naturwissenschaften, 79*, 428–431.

Przybyszewski, A. W. (1991). An analysis of the oscillatory patterns in the central nervous system with the wavelet method. *Journal of Neuroscience Methods, 38*, 247–257.

Sakai, H. M. & Naka, K.-I. (1990). Dissection of the neural network in the catfish inner retina. V. Interactions between NA and NB amacrine cells. *Journal of Neurophysiology, 63*, 120–129.

Stocker, J. J. (1950). *Nonlinear vibrations in mechanical and electrical systems.* New York: Interscience.

Wunk, D. F. & Werblin, F. S. (1979). Synaptic inputs to the ganglion cells in the tiger salamander retina. *Journal of General Physiology, 73*, 265–286.

Acknowledgements—We thank Professor F. Takens for his stimulating interest in this work. Dr B. Braaksma and Professor J. Grasman helped us with the analysis of the van der Pol equation. We also thank Professor W. Szlenk for his comments on an earlier version of the manuscript. This work was supported by the Biophysics Foundation of the Netherlands Organization for Scientific Research (NWO).